Broad Lane, Sheffield S3 7HQ
Telephone: 0114 289 2000
Facsimile: 0114 289 2500

HEALTH & SAFETY LABORATORY

A study of the consequences of leaks from gas turbine power plant sited in a turbine hall

HSL/2000/19

Project Leader: Dr C J Lea

Authors: Dr M J Lewis & Dr C J Lea

Fire & Explosion Group

Summary

Objectives

Natural gas is now widely used to fire large industrial gas turbines for power generation. It is common practice to house gas turbines inside enclosures to suppress noise and provide a controlled operating environment. However, in the event of a fuel leak, the enclosure may facilitate the build-up of a flammable gas cloud.

Two types of enclosure exist: Relatively small acoustic enclosures and much larger turbine halls. In this study the issues and concerns arising from gas leaks in large turbine halls are investigated, with the aim of identifying the associated hazards and in particular highlighting any differences in strategy for mitigating the effects of gas leaks in comparison to acoustic enclosures.

To meet these objectives a combined measurement and Computational Fluid Dynamics (CFD) modelling study has been applied to simulate the consequences of gas leaks in a large turbine hall. For the purposes of this study one of the gas turbine halls at the Didcot B station, owned by National Power, has been investigated - since it embodies features likely to be representative of this type of installation.

Main Findings

Flow measurements in the hall show that the flow speed and temperature are significantly influenced by external atmospheric conditions. This results from a combination of factors, which are nevertheless likely to be encountered at other installations of this type. The net effect, however, is that it becomes more difficult to control the flow conditions in a large turbine hall than in an acoustic enclosure.

This uncertainty in flow conditions poses problems when CFD modelling is applied to a large turbine hall, since it becomes more difficult to measure and specify representative boundary conditions. Indeed upon comparison of the measured and simulated background flow at points around the hall, it was found that the CFD model under-predicted flow speed. This is likely to be a consequence of uncertainties in the specification of boundary conditions, the omission of the influence of external conditions - i.e. wind gusts and leakage into the hall at doors etc., coupled to uncertainties arising from the CFD numerical and physical sub-models. The CFD modelling of flow conditions in a large turbine hall is thus more challenging than its application to acoustic enclosures.

Overall, it appears that potential worst case gas leaks in turbine halls are less likely to lead to the build-up of flammable clouds which would cause significant over-pressure than is the case for acoustic enclosures. This is a direct consequence of similar overall ventilation rates and detection levels in the two cases, which leads to a similar-sized worst case leak, yet sited in a much larger volume. However the study indicates that dilution ventilation is also less appropriate as a basis for safety in large turbine halls. Instead the focus is shifted towards gas detection.

This study indicates that detectors located immediately above turbine combustors will be triggered by a just-detectable leak after approximately one minute. However this finding is

based upon a necessarily limited set of simulations. Other leaks which could be foreseeable may result in the build-up of a gas cloud in a part of the hall remote from detectors, with a subsequent increase in the time to detection. In this case the siting of deflectors, designed to direct the passage of a potential gas leak towards the detectors may be beneficial. This measure has been implemented at the Didcot B station.

Main Recommendations

There is more uncertainty in the CFD modelling of flow and gas leaks in large turbine halls than is the case for turbines housed in acoustic enclosures. The CFD results presented in this study should therefore be regarded with some caution. The following work would help reduce this uncertainty:

It would be useful to investigate the sensitivity of the gas cloud size and location to the prescribed hall boundary conditions to determine the extent to which it is acceptable to apply design conditions as CFD boundary conditions.

There appears to be considerable uncertainty associated with the CFD modelling of high pressure gas leaks in congested regions when the leak is treated using a point source approach and the congestion is modelled using a sub-grid porosity approach. It is recommended that this area of uncertainty be investigated to determine the root cause and identify solutions.

The consequences of installing deflectors should be quantified. This would involve the CFD modelling of gas leaks in the local vicinity of deflectors. This task appears to be more amenable to a CFD-based approach than that of modelling flow and gas dispersal throughout the entire turbine hall.

Contents

1. INTRODUCTION

In recent years there has been a rapid growth in the use of natural gas as a fuel for power generation. This fuel is used to fire large industrial gas turbines, where power output is approaching 300 MW for a single machine. It is common practice to house gas turbines inside enclosures to suppress noise and also to provide a controlled operating environment. However, in the event of a fuel leak the enclosure may facilitate the build up of a flammable gas cloud.

Two types of enclosure exist. The first is a relatively small enclosure which encases the turbine and is typically of volume 1000m^3; these are generally referred to as acoustic enclosures. In this case the hazards associated with gas leaks depend critically on the performance of the enclosure's ventilation system in ensuring that gasbuild-up does not occur. For this type of enclosure, guidelines for a maximum acceptable gas cloud size are available (Santon, 1997). The guidelines aim for "Dilution from pure gas to 50% LEL within a volume of 0.1% of the net volume of the enclosure, from a leak which would trigger gas detection". The basis for this criterion is that ignition of such a cloud is unlikely to create an over-pressure sufficient to damage the enclosure and to pose a risk of injury to persons outside. Optimisation of ventilation system performance is typically achieved by a combination of Computational Fluid Dynamics (CFD) modelling and physical tests.

In the second type of enclosure the turbine is positioned in a much larger hall, typically of volume 10,000m^3 or more. In this case, provision of a strategy to deal with a gas leak is not so obvious. Due to the massive volume of the hall, the gas cloud would have to be very large to produce a significant over-pressure. However, even though ventilation is provided, it is typically nominal in relation to the hall volume, and therefore the time for a gas leak to be detected could be large.

At present most industrial gas turbines are housed in acoustic enclosures and guidance on mitigating the consequences of gas leaks is already well-developed (Santon, 1997). The issues and concerns arising from gas leaks in large turbine halls are less clear, simply because there are relatively few installations of this type in existence. The objectives of the present study are thus:

- To identify hazards associated with leaks in turbine halls and highlight any differences in strategy for mitigating the effects of gas leaks in comparison to acoustic enclosures.

- To attempt to quantify the cost-benefits of housing in a large turbine hall compared to an acoustic enclosure.

- To bring the above to the attention of the power generation industry.

To meet these objectives, CFD modelling has been applied to simulate the consequences of gas leaks in a large turbine hall. For the purposes of this study one of the gas turbine halls at Didcot B has been investigated since it embodies features likely to be representative of this type of installation. The Didcot B station is owned by National Power.

Figures 1 to 7 show some of the main features at Didcot B. Figure 1 shows one of the two turbine halls, each of which house two turbines; Figures 2 to 4 show details of the gas supply pipework around the turbines and gas detectors above the silo combustors; Figures 5 to 7 illustrate the inlets and exhaust ducts for ventilating air to the hall.

The work has been carried out in collaboration with National Power plc and builds upon an initial study of potential gas leaks in the Didcot B station by AEA Technology (Sinai and Hoyal, 1997).

2. METHODOLOGY

A combined CFD modelling and on site measurement study was undertaken. Measurements were made with the intention of providing boundary conditions for the CFD modelling and data under normal operating conditions to investigate the applicability of the CFD. Measurements of both temperature and velocity were taken at strategic points inside the enclosure, as well as at the inlet ducts. Details of the measurements taken are reported and discussed in Appendix A.

The Didcot B station comprises two turbine halls, each housing two gas turbines. One of the halls houses turbines with annular combustors and the other houses turbines with silo combustors. The annular combustors are positioned circumferentially around the turbine, whereas the silo combustors are located at either side of the turbine and approximately mid-way along its length - visible in Figures 1, 2 and 4.

In the initial study by AEAT the modelling was based on the annular combustor gas turbines. However during the present study only the silo combustor gas turbine hall was operational. Furthermore, National Power were able to supply thermographic data on surface temperatures for the silo combustor gas turbines. It was thus agreed that the silo combustor gas turbine hall would be the subject of the present study.

A CFD model of the turbine hall was constructed. Initially, normal operating conditions were simulated to establish the background ventilation state. Gas leaks were then introduced into this background flow for both hot and cold running conditions - allowing an indication to be gained of the effect of leaks during normal operation and following turbine start-up from cold. Simulations were undertaken for steady-state conditions and in a time-dependent manner to provide information on gas build-up over time and the approximate time to detection.

Comparisons are made with the results of the earlier study by AEAT and with measurements taken on site.

The approach taken in the CFD modelling is detailed below. All simulations were undertaken using CFX4.2, a mature, commercially-available software package developed and marketed by AEA Technology.

2.1 Computational domain and grid

A multi-block mesh was created to represent the turbine hall. The model resolves the major features, such as the turbine casing, in an explicit fashion. Smaller features, such as pipework, are accounted for by imposing a porosity-based sub-grid model.

The features that have been represented explicitly are:

- the whole enclosure, including both turbines and the generator bays.
- the turbine casing.
- an air-cooled electric motor located at the side of each turbine and the concrete plinths on which they sit.
- the location and size of the thirteen inlet ducts.
- the location and size of the four extract ducts.
- the partitions between the turbine hall and the generator bays
- an approximate representation of the generators

These features are illustrated in Figure 8, which show those parts of the geometry explicitly resolved by the CFD mesh. The regions within which the small-scale structures have been modelled using a porosity-based approach are depicted in Figure 9.

The mesh is made up of 96 blocks and possesses approximately 370,000 cells. Figures 10 and 11 illustrate the grid disposition in a vertical and horizontal plane respectively.

2.2 Boundary conditions

2.2.1 Flow

The measured ventilation flow at inlets and in the main part of the hall was strongly influenced by external conditions. Details can be found in Appendix A, but in summary the measured flow at particular locations was subject to large fluctuations about a mean, whilst the mean would vary depending on the day measurements were taken. This behaviour is almost certainly caused by interaction of the external windfield on the forced ventilation flow in the hall.

Simulations of normal operating conditions were thus undertaken in which either the measured flow or the design ventilation flow (a total of $28m^3/s$) were applied as boundary conditions at the 13 inlets to the hall. Sensitivity to these two sets of boundary conditions was investigated and is discussed in Section 3.2. For both cases the four extract ducts were defined as ‘mass flow boundaries’, so as to conserve overall mass flow through the hall.

No-slip smooth wall turbulent boundary conditions were applied at all solid boundaries.

2.2.2 Thermal conditions

The flow into the enclosure was set at the measured ambient temperature during the visit on 16/6/98. The wall thermal boundary condition was assumed to be adiabatic, but a further condition was investigated in which the walls of the enclosure were maintained at the measured ambient temperature (see Section 3.2).

Thermographic images provided by National Power show the variation of surface temperature over the turbines. These are insulated except at the ends of the silo combustors. The thermographic data was used to derive a simplified surface temperature distribution for the CFD model: The end faces of the silo combustors are un-insulated and a uniform temperature of 300°C was specified; For the remaining surfaces of the turbine a mean value of 120°C was specified.

2.2.3 Gas leak source

Gas leaks were implemented in the model as sub-grid point sources of methane. This has the advantage that the leak can be positioned arbitrarily without the need for mesh regeneration. Well-established empirical correlations for under-expanded jets are used to calculate model sources of mass, momentum, and enthalpy, based upon the leak position, hole area and direction and the fuel supply temperature and pressure (Ewan and Moodie, 1986; Sinai & Hoyal, 1997).

2.3 Physical sub-models

A standard buoyancy modified k-ε turbulence model was used (Rodi, 1978). The value of 1.0 was assigned to C_3 in the buoyancy term of the turbulence dissipation equation. An additional scalar transport equation was solved for the gas source, modelled as 100% methane.

Weakly compressible flow was assumed, in which variations in pressure do not affect the density. This is a valid assumption for low mach number buoyant flows of the type generally encountered here - remembering that the highly-compressible near-source region is not explicitly resolved. The gaseous mixture was assumed to be transparent to thermal radiation. Radiative exchange was thus not modelled.

Congested regions were represented by imposing sub-grid resistance, heat transfer and turbulence generation source and sink terms, following the approach adopted by Sinai & Hoyal (1997). The resistance tensor was assumed to be isotropic. The model used in-line correlations of pressure drop, with a characteristic pitch of 0.5m and a tube diameter of 0.2m (McAdams, 1954). A heat source has been prescribed in the resistance regions to represent heat transfer from hot pipework. It is evaluated using the local fluid conditions and the local 'pipe' temperature, assumed to be 120°C, with the pipe area per unit computational volume defined by the pipe pitch and diameter. Clearly, these represent simplifications of the real plant, and while greater detail may be possible, this is beyond the scope of the current project. It should be noted that these assumptions introduce uncertainty into the simulation since large regions of intricate pipework are represented crudely. The flow is averaged in these regions and detail is lost, which forms the basis of the resulting uncertainty.

2.4 Numerical sub-models

The CCCT higher-order differencing scheme was employed throughout in order to reduce the deleterious effects of numerical diffusion. Steady-state solutions were achieved with the use of under-relaxation values of 0.4 and false time steps of 1e-4 s. Transient simulations used a real time step of 1 s. It should be emphasised that it proved difficult to obtain a converged solution because the hall is very large and has a small ventilation rate, thus there is no strongly defined flow direction. However this strategy did produce reasonably well-converged results. The global mass residual was used to judge convergence, in which the residual was typically less than 0.1% of the mass flow rate into the hall. The real time taken to complete a transient simulation was of the order of five days.

2.5 Simulated scenarios

Table 1 outlines the reported simulations.

The first scenario allows a comparison to be drawn between measured and simulated flow conditions in the hall and helps to investigate the validity of the CFD model. The second scenario is a repeat of a case simulated by AEAT, to explore consistency in the modelled results. The release rate is that used by Sinai & Hoyal (1997).

The remaining scenarios investigate the consequences of a leak which would just trigger gas detectors set to alarm at 10% of the Lower Explosive Limit for well-mixed conditions close to the exhaust from the hall. The leak location is at the lower end of a silo combustor, directed towards the floor underneath the axis of the turbine.

Table 1: Scenarios simulated

Scenario	Operat-ing Status	Turbine Temperature	Steady / Transient	Leak Rate (kg/s)	Gas Leak Description	Leak Position	Leak Direction Cosines
1	Normal	Hot	Steady	None	None	-	-
2	Normal	Hot	Steady	3.19E-01	Case 4 - Sinai & Hoyal, 1997	20, 2.4, 8.3	0.0, -0.7071, 0.7071
3	Normal	Hot	Steady	1.60E-01	Lower end of silo combustor towards the floor beneath the axis of the turbine (Figure 13)	15, 2.70, 7.7	0.7071, -0.7071, 0.0
4	Normal	Hot	Transient	“	“	“	“
5	Start-up	Cold	Steady	“	“	“	“
6	Start-up	Cold	Transient	“	“	“	“

3. BACKGROUND VENTILATION: SCENARIO 1

3.1 Base case

In this case, steady-state flow rates at each of the inlets were set according to the design specification, giving a total volume flux through the hall of $28m^3/s$. The walls are assumed to be adiabatic.

Table 2 compares the simulated and measured flow speeds at positions mapped with the ultrasonic anemometer, deemed to be the most reliable of the flow measurements. See Appendix A for details.

Table 2 Comparison of simulated and measured flow speeds, Scenario 1

Position	Height (m)	Simulated flow speed (m/s)	Measured minimum flow speed (m/s)	Measured mean flow speed (m/s)
1	5.8	0.03	0.02	0.15
1	9.8	0.03	0	0.17
3	5.8	0.22	0.12	0.23
3	9.8	0.06	0.05	0.19
4	5.8	0.09	0.11	0.36
4	9.8	0.02	0	0.23

The simulated flow speeds are generally within the lower bound of the ultrasonic anemometer measurements, but well below the measured mean velocities. However one of the most notable features observed during the measurement programme was the very large fluctuation in flow speeds in the hall. It became clear during the course of the measurements that this was largely due to the influence of external conditions. Thus a gust of wind outside the hall could result in local increases in flow rate through the ventilation inlets. This effect is not represented in the model. In addition there are other areas over which flow can enter the hall - gaps below roller shutter doors, access routes into the enclosure, etc., which also add to the measured flow but again are not represented in the model.

On balance it is therefore not surprising that the simulation under-predicts measured mean velocities, since these will be skewed towards the velocity maxima by local gusts.

The predominant flow pattern consists of a hot plume rising above the gas turbines setting in motion a weak recirculating flow confined to the upper part of the hall. See Figure 14.

The simulated temperature field on a vertical plane through the centre of the silo combustors is shown in figure 15. The simulated flow is strongly stratified, in agreement with observations. The predicted temperature close to roof level in the hall is ~20^0C above ambient, and approximately 2^0C below measured temperature rises at this location. This indicates that the overall heat balance in the hall is adequately modelled.

3.2 Sensitivity to boundary conditions

Measurements in the turbine hall indicate that the simulated flow could well be sensitive to the imposed boundary conditions. A series of sensitivity tests were thus undertaken to the ventilation and wall thermal boundary conditions:

- A. Upper limit of the measured inlet velocities on 16/6/98.
- B. Lower limit of the measured inlet velocities on 16/6/98.
- C. Design ventilation conditions, but ambient temperature walls.

Tests A and B did not greatly alter the gross flow character. However simulated values of flow speed tended to increase, particularly so for Test A, although flow magnitudes were still generally less than measured mean values at point locations in the hall.

Test C also leads to an increase in the simulated flow speed, largely due to the presence of complex recirculating flows as air which is cooled at the walls sinks. In this case the overall flow character is changed and stratification is reduced.

The flow in the hall is sensitive to the imposed ventilation and wall thermal boundary conditions. Unfortunately there is no strong case for selection of one set of conditions over another, especially given the uncertainties introduced by the influence of conditions external to the hall - which cannot readily be represented in the model and will vary from day to day. The task of selecting appropriate boundary conditions is thus very difficult.

A decision was thus taken to apply the design ventilation flows as inlet boundary conditions coupled to an adiabatic wall condition.

4. GAS LEAKS UNDER NORMAL OPERATING CONDITIONS

4.1 Scenario 2

The leak position and orientation is as per AEAT's simulation of the annular combustor gas turbine, i.e. underneath the turbine and directed towards the partition leading to the generator bay. Although this leak position is less credible for silo combustor gas turbines, it does provide an opportunity to compare gas cloud sizes with those from AEA Technology's initial study.

Unfortunately a direct comparison is misleading, since there are substantial differences in the two approaches. Thus the earlier work by AEAT models one half of the hall and does not include the effects of forced ventilation. In addition there will be differences in the CFD grid and numerical approach, etc.

Importantly, there are also key differences in the location of porous regions representing pipework etc. AEAT model porous regions arranged annularly around the turbines. In the present work porous regions are defined underneath the length of the turbines and above the turbines, Figure 9. As a result, the gas leak is defined to be directly within the porous region, whereas in the AEAT study the leak source lies outside the porous region.

Figure 16 shows an iso-surface at 50% LEL for the AEAT simulation. Table 3 below shows that this encloses a volume of 40.5m^3. In the present study the equivalent cloud volume is very much larger, ~1023m^3, Figure 17. Interestingly, if porous regions are removed the cloud size drops dramatically to ~28m^3, Figure 18. In this case a comparison of Figures 16 and 18 shows that the location and shape of the cloud is very similar to that predicted by AEAT.

Table 3: Simulated gas cloud volume

Scenario	Porous Regions	Steady-state volume enclosed by 50 % LEL iso-surface
AEAT Case 4	N/A	40.5 m^3
2	No	~28 m^3
2	Yes	~1,023 m^3
3	No	~7 m^3
3	Yes	~10 m^3
5	No	~7 m^3

It seems that when the leak is located within a defined porous region, the vast majority of the initial momentum is lost in the near vicinity of the source. Since momentum is ultimately responsible for the relatively rapid mixing and diffusion of the gas leak close to the source, any reduction will result in lower levels of mixing and dilution. Further dilution and transport of the gas away from the source can then only be achieved by the background ventilation flow and the natural buoyancy of the mixture, processes which are apparently less effective in comparison to jet-induced mixing.

In practice even if a leak does occur in a congested region, then initial momentum seems unlikely to be lost so rapidly. Impingement and interaction with obstacles will ultimately result in some loss of momentum, but in the very near-source region it is conjectured that the main effect will be to divert the gas jet. The very large cloud size predicted in this case should thus be treated with some scepticism. It is more likely to be a consequence of the crude modelling of both the source and unresolved obstacles, than a real effect. If this proves to be the case, then the cloud size and shape as predicted by AEAT and HSL (without porous regions) are consistent.

Fortuitously, the site of potential gas leaks for silo combustor gas turbines is outside the defined porous region. It is shown below that this source of uncertainty is then very much reduced.

4.2 Scenario 3

It was agreed with National Power that possibly the most likely position for a gas leak was from the high pressure supply pipework close to the silo combustor end-plate. The direction of the leak was chosen so as to represent a possible worst case, that is towards a region of relatively low flow speeds and away from gas detectors. It was thus agreed that the leak was to be located at the lower end of a silo combustor end-plate, directed at an angle of 45^{o} to the horizontal and towards the floor underneath the turbine. For a silo combustor gas turbine this represents a more realistic leak size, position, and orientation than that reported above.

Simulations were undertaken both with and without porous congested regions imposed beneath the turbines. The resulting gas clouds sizes, defined by the 50% LEL iso-surface, are only slightly different (see Table 3), certainly much smaller than those seen in scenario 2. There are two main reasons for this: Firstly, the size of the gas leak is smaller; Secondly, the leak source is not located within the porous congested region, and momentum induced mixing has to a large degree already occurred prior to the interaction of the gas cloud with the congested region. Importantly both cloud sizes are smaller than the criteria based on 0.1% of the enclosure volume (Santon, 1997). Figure 19 shows the 50% LEL iso-surface for this scenario, in the absence of a porous region below the gas turbine.

At Didcot B the gas detectors are set to alarm at 10% LEL. Detectors are sited approximately two metres above the ends of the silo combustors and at roof level close to the extract ducts. Analysis of the CFD results shows that the volume of the gas cloud in which concentration exceeds 10% LEL is very large, see Figure 20. There are many detectors which would be enveloped by this cloud.

4.3 Scenario 4

To investigate the time to detection, transient simulations were undertaken. The time-dependent build-up of gas was thus modelled for the conditions as defined in scenario 3.

Analysis of the results shows that gas initially builds up below the turbine, as well as underneath and beyond the opposite silo combustor, see Figure 21. After a period of approximately one minute gas envelops the opposite silo combustor, Figure 22, and rises upwards. It can then be inferred that detection occurs.

5. GAS LEAKS UNDER START-UP CONDITIONS

Possibly the most likely time for a gas leak to occur is following a routine shut down for maintenance. Upon start-up the gas turbines will be cold and therefore the natural convection driven flow above the turbines is not present. This will change the flow patterns inside the hall, with the possibility that any build-up of gas will take longer to reach and trigger the gas detectors. Scenario 3 and 4 were therefore repeated with cold gas turbines - with all walls set to ambient temperature.

5.1 Scenario 5

Close to the leak source the behaviour of the gas is almost identical to that seen under normal operating conditions, see Figure 23. The momentum of the jet dominates and the volume enclosed by the 50% iso-surface is essentially the same as that of scenario 3, at ~$7m^3$.

Further from the jet source - where momentum has decayed, the cloud builds-up and rises mainly in the middle of the hall, driven by weak forced convection and natural buoyancy, see Figure 24. This is rather different from scenario 3, in which gas becomes entrained in the hot plume rising above the gas turbine.

The 10% LEL iso-surface again fills a substantial volume of the entire hall and envelops several gas detectors.

5.2 Scenario 6

The transient simulation confirms that under start-up conditions the gas cloud tends to build-up in the centre of the hall once momentum has decayed. Since the hall is not stably-stratified, gas is free to rise towards the roof, reaching the extract ducts some 30 seconds later than under normal operating conditions. The 10% LEL iso-surface is again of large volume, with the result that the time to detection is still approximately one minute.

6. DISCUSSION

The measured flow in the Didcot B turbine hall was found to be significantly influenced by external atmospheric conditions. This results from a combination of factors: a modest force-ventilated air change rate - albeit at $28m^3/s$ substantial in absolute terms; the need to draw ventilating air from directly outside the hall; practical difficulties in ensuring that other sources of flow into or from the hall - such as at roller shutter doors, are controlled. It should be stressed that these factors are very likely to be significant at other installations of this type. The net effect, however, is that it becomes more difficult to control the flow conditions in a large turbine hall than in an acoustic enclosure.

This uncertainty in flow conditions poses problems when CFD modelling is applied to a large turbine hall, since it becomes more difficult to measure and specify representative boundary conditions. In this work a number of alternative boundary conditions were examined, but in the absence of any clear benefit from one set over another, the design ventilation conditions were ultimately used, coupled to assumed adiabatic external walls.

Upon comparison of the measured and simulated background flow at points around the hall, it is clear that the model under-predicts flow speed. It is not easy to isolate the reasons for this. It is certainly likely to be in part a consequence of the omission of the influence of external conditions - i.e. wind gusts and leakage into the hall at doors etc.

In addition, there will be numerical and physical errors in the model which could contribute to the underprediction. Thus the hall is resolved with a substantial number of grid cells, 370,000, but even so the size of the hall means that the grid cell spacing is still quite large. Some initial simulations were undertaken on a coarser grid comprising 220,000 cells. Refinement to the present 370,000 cells did bring the simulated flow speeds closer to measurements. It is probable that further grid refinement would result in further improvements. Flow in the hall is also extremely complex - being driven by both natural and weak-forced convection, and can only be expected to be crudely resolved by a k-ε turbulence model.

The CFD modelling of flow conditions in a large turbine hall is thus more challenging than its application to acoustic enclosures.

One consequence of the under-prediction in background flow speed is that it implies that the rate at which dilute gas is transported by the background flow will also be under-predicted. That is, simulated times to detection could be greater than occur in reality. In this respect the model could be regarded as conservative.

The predicted volumes of gas enclosed by the steady-state 50% LEL iso-surface are generally substantially less than the criterion based on 0.1% of the hall volume, under both normal operating and cold start-up conditions. The reason for this is that the 50% LEL cloud volume is, for a given leak source and in the absence of re-entrainment, largely determined by jet-induced turbulent mixing. An exception was seen in Scenario 2 in circumstances in which the gas leak is positioned inside a defined porous region, in which case the 50% LEL iso-surface was very large. However the discussion in section 4.1 makes clear that there is considerable doubt as to the credibility of this result, which reflects a particular uncertainty in the CFD modelling and requires further study.

If ignited, leaks such as those simulated would result in a deflagration, probably followed by a jet fire. It appears that potential ‘worst case’ gas leaks in turbine halls are less likely to lead to the build-up of flammable clouds which could cause significant over-pressure than is the case for acoustic enclosures. This is a direct consequence of similar overall ventilation rates and detection levels in the two cases, which leads to a similar-sized worst case leak, yet sited in a much larger volume.

The size of the steady-state 10% LEL iso-surface is, in all scenarios simulated, very large. It fills a substantial volume of the entire hall and encompasses several detector locations. Detection can thus be assumed to have occurred. However the size of the hall is such that the time to detection could be large. There is thus a strong case for transient simulations to be undertaken for gas leaks in turbine halls to determine the time to detection, a situation which is less likely to be of concern in acoustic enclosures.

Transient simulations were undertaken in the present study and indicate that for the leaks investigated the time to detection is approximately one minute, for both normal operating and cold start-up conditions.

It is interesting to note that when transient simulations were undertaken for normal operating conditions, section 4.3, the gas initially appears to be confined below the level at which temperature stratification occurs in the hall. It is only when gas becomes entrained into the hot plume generated by the operating turbine that gas begins to be transported into the hotter upper parts of the hall and past detector locations. Certainly the cloud will be weakly buoyant at concentrations of order 10% LEL, so initial confinement of the cloud to the lower levels of the hall by temperature stratification seems plausible.

In contrast, the behaviour of the gas cloud under start-up conditions is different, in that once momentum has decayed the cloud builds-up and rises mainly in the middle of the hall, driven by weak forced convection and natural buoyancy, reaching the extract ducts some 30 seconds later than under normal operating conditions.

In general, compared to acoustic enclosure installations, forced ventilation flow in a turbine hall can be expected to be much smaller relative to the hall volume, i.e. lower air change per hour. As a consequence, natural convection driven flow will be more dominant. The overall flow patterns are thus potentially substantially different under hot and cold running conditions. In principle this could mean that the route of gas past a detector and times to detection could be very different. Although times to detection were in fact found to be similar in this study, it does suggests that it becomes more important to consider the effects of both normal operating and start-up conditions for turbine halls than is the case with acoustic enclosures.

The leaks investigated in this study were generally directed underneath a gas turbine and towards the silo combustor on the opposite side of the machine, above which are sited gas detectors and which are the first to 'see' the gas cloud. Indeed the extent of the computed 10% iso-surface suggests that the exact location of gas detectors may not be critical. However this finding is based on a necessarily limited set of simulations, which are likely to be less reliable than similar simulations for acoustic enclosures. There remains a possibility that a leak could be oriented directly towards the centre of the hall, in which case it may not be detected for some time.

To mitigate this possibility it would in principle be possible to site additional detectors in this location. However an alternative strategy exists: The fitting of deflectors designed to direct the passage of a potential gas leak towards detectors. This strategy has been implemented at the Didcot B station. Careful design of deflectors is needed to ensure that they do not promote build-up of large volumes of gas through confinement of the flow and re-entrainment. The design and assessment of performance of deflectors should be amenable to CFD modelling.

7. CONCLUSIONS

A combined measurement and CFD modelling study has been undertaken, examining potential gas leaks in a large turbine hall, with the main objective being to highlight differences in strategy for dealing with gas leaks in comparison to housing in an acoustic enclosure. For the purposes of this study one of the turbine halls at the Didcot B station, owned by National Power, has been investigated - since it embodies features likely to be representative of this class of installation.

Flow measurements in the hall showed that the flow speed and temperature were significantly influenced by external atmospheric conditions. This results from a combination of factors, which are nevertheless likely to be encountered at other installations of this type. The net effect, however, is that it becomes more difficult to control the flow conditions in a large turbine hall than in an acoustic enclosure.

This uncertainty in flow conditions poses problems when CFD modelling is applied to a large turbine hall, since it becomes more difficult to measure and specify representative boundary conditions. Indeed upon comparison of the measured and simulated background flow at points around the hall, it was found that the CFD model under-predicted flow speed. This is likely to be a consequence of uncertainties in the specification of boundary conditions, the omission of the influence of external conditions - i.e. wind gusts and leakage into the hall at doors etc., coupled to uncertainties arising from the CFD numerical and physical sub-models. The CFD modelling of flow conditions in a large turbine hall is thus more challenging than its application to acoustic enclosures.

Overall, it appears that potential worst case gas leaks in turbine halls are less likely to lead to the build-up of flammable clouds which would cause significant over-pressure than is the case for acoustic enclosures. This is a direct consequence of similar overall ventilation rates and detection levels in the two cases, which leads to a similar-sized worst case leak, yet sited in a much larger volume. However the study indicates that dilution ventilation is also less appropriate as a basis for safety in large turbine halls. Instead the focus is shifted towards gas detection.

This study indicates that detectors located immediately above turbine combustors will be triggered by a just-detectable leak after approximately one minute. However this finding is based upon a necessarily limited set of simulations. Other leaks which could be foreseeable may result in the build-up of a gas cloud in a part of the hall remote from detectors, with a subsequent increase in the time to detection. In this case the siting of deflectors, designed to direct the passage of a potential gas leak towards the detectors may be beneficial. This measure has been implemented at the Didcot B station.

8. RECOMMENDATIONS FOR FURTHER WORK

A sensitivity analysis shows that the simulated background flow conditions in the hall depend strongly on the prescribed boundary conditions, but that these are difficult to ascertain with certainty. However no simulations were undertaken in which the sensitivity of the gas cloud to boundary conditions was examined. It would be useful to investigate the sensitivity of the gas cloud size and location to determine the extent to which it is acceptable to apply design conditions as CFD boundary conditions.

There appears to be considerable uncertainty associated with the CFD modelling of high pressure gas leaks in congested regions when the leak is treated using a point source approach and the congestion is modelled using a sub-grid porosity approach. This finding is likely to be applicable to other situations, such as leaks in offshore process modules or onshore chemical process plant. It is recommended that this area of uncertainty be investigated to determine the root cause and identify solutions.

The consequences of installing deflectors should be quantified. This would involve the CFD modelling of gas leaks in the local vicinity of deflectors. This task appears to be more amenable to a CFD-based approach than that of modelling flow and gas dispersal throughout the entire turbine hall.

9. ACKNOWLEDGMENTS

This work was funded by the Field Operations Division of the UK Health & Safety Executive. The authors would like to acknowledge the assistance and co-operation of National Power plc, in particular Dr P Stephenson, for arranging access to and information on the Didcot B station. The contribution of Dr A Thyer, R Hambleton and J Saunders of the Health and Safety Laboratory, in undertaking the reported measurements, is also gratefully acknowledged. Finally the authors would like to thank RWE Innogy, the current owners of Didcot B, for allowing this report to be published on the internet.

10. REFERENCES

Ewan B C R and Moodie K (1986)
Structure and Velocity measurements in under-expanded jets
Combustion Science and Technology, Vol 45, pp 275-288.

McAdams W H (1954)
Heat Transmission, Third Edition
McGraw-Hill Kogakusha.

Rodi W (1978)
Turbulence models and their application in hydraulics - a state of the art review.
SFB Report 80/T/125, University of Karlsruhe.

Santon R C (1997)
Explosion Hazards at Gas Turbine Driven Power Plants
Proc. IMechE Seminar on Prevention and Control of Gas Explosions in CCGT and Steam Plants, 8 October 1997, London.

Sinai Y L and Hoyal B (1997)
CFD Investigation of Gas Dispersion at Didcot ’B’ Power Station
AEAT/CFDS/CONS/REP97/407.1

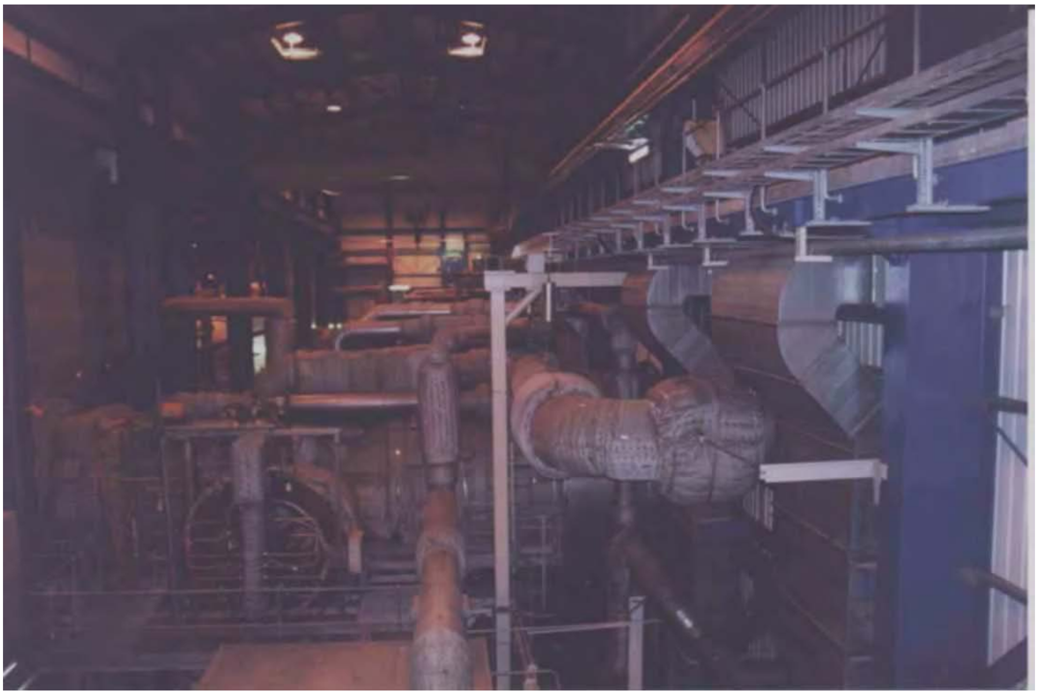

Figure 1: The gas turbine hall

Figure 2: Pipework above a gas turbine.

Figure 3: Pipework and structure beneath a gas turbine.

Figure 4: Gas detectors above a silo combustor.

Figure 5: Inlet ducts with horizontal baffles, as found in the generator bays

Figure 6: Vertical inlet ducts, as found on the long wall of the hall.

Figure 7: Roof extract ducts.

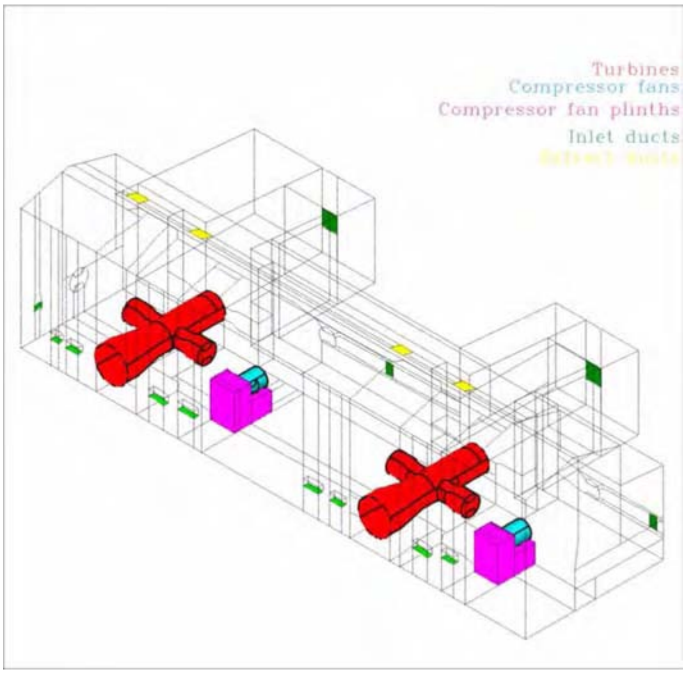

Figure 8: Features of the turbine hall resolved by the CFD grid .

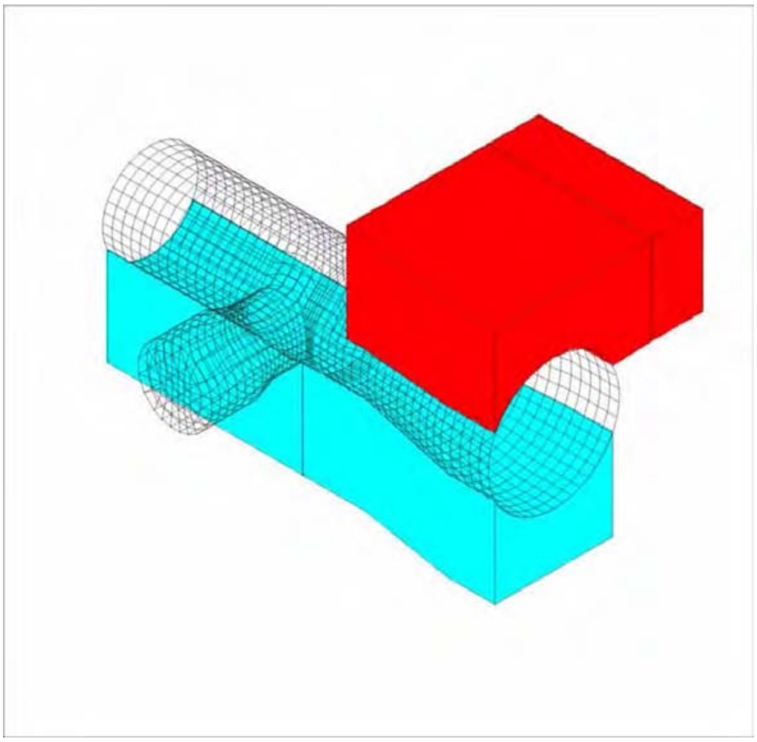

Figure 9: Congested regions above and below the turbines represented using a porosity based sub-model.

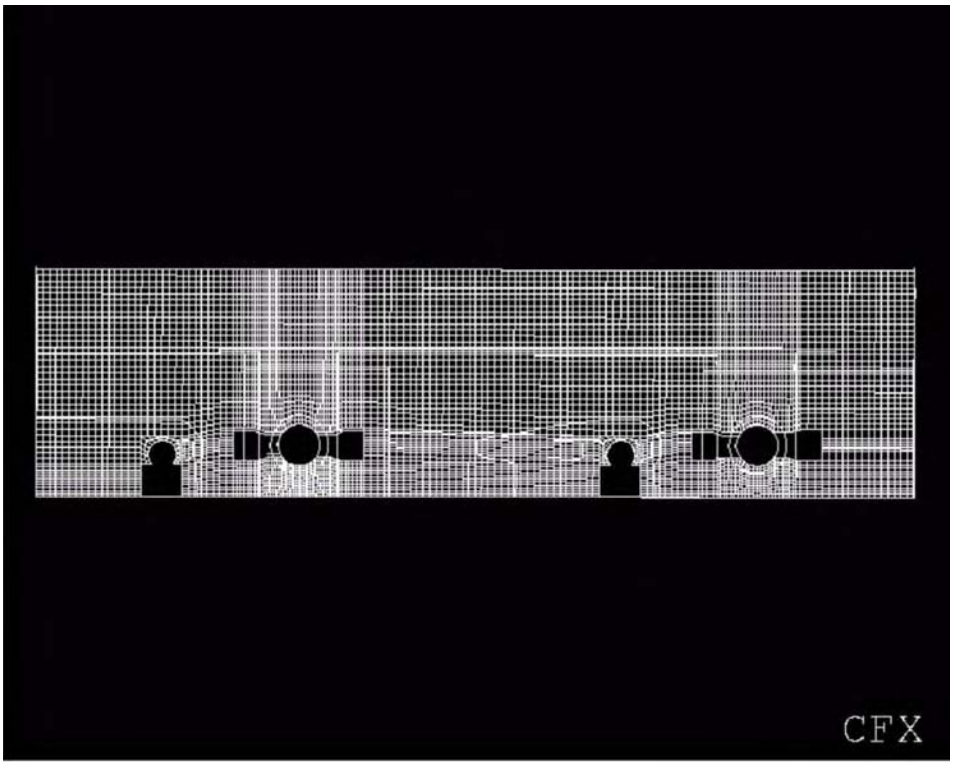

Figure 10: Vertical plane through the grid along the axis of the silo combustors.

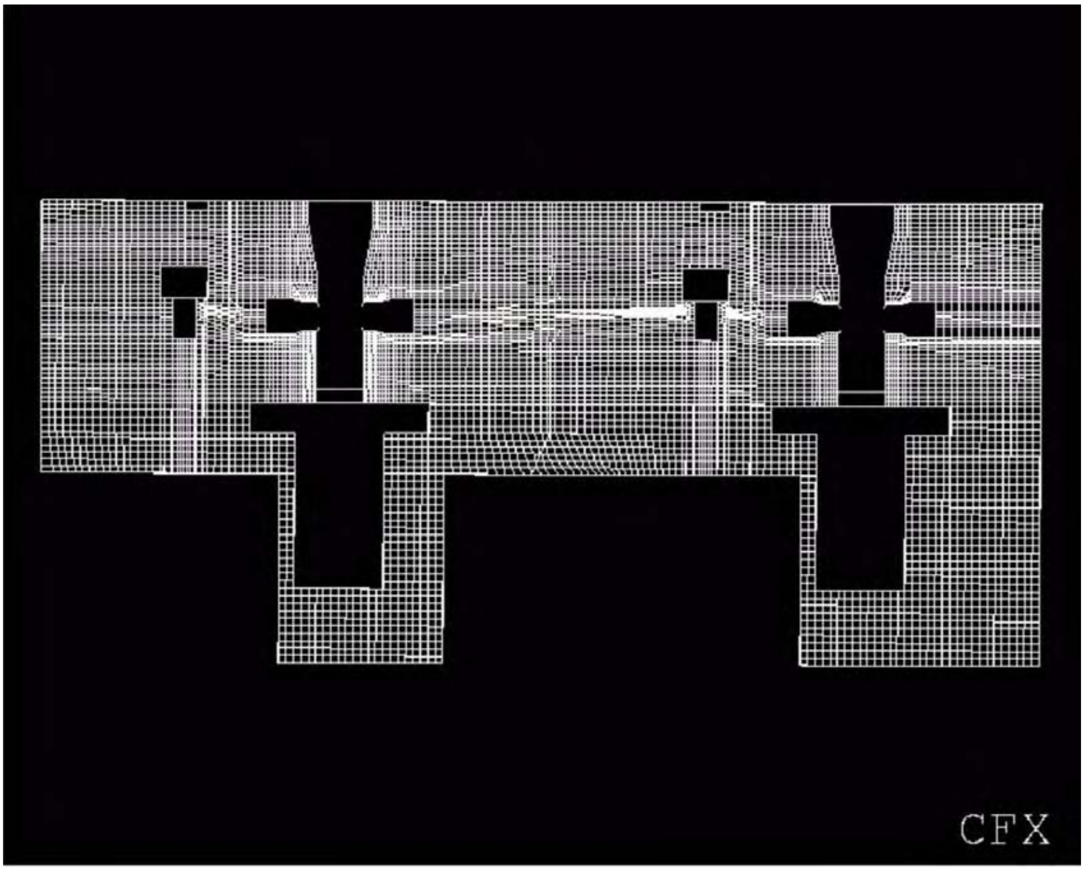

Figure 11: Horizontal plane through grid along the axis of the silo combustors.

Figure 12:Indication of gas leak location and orientation for scenario 2.

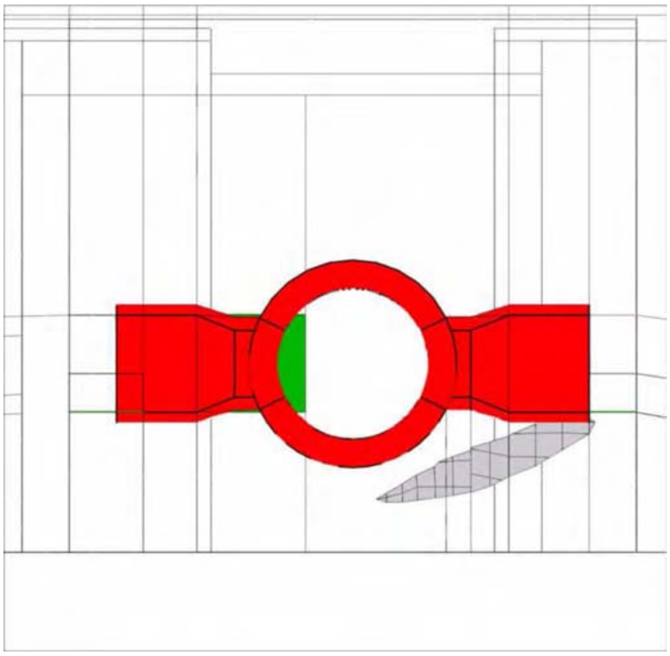

Figure 13: Indication of gas leak location and orientation for scenarios 3 to 6.

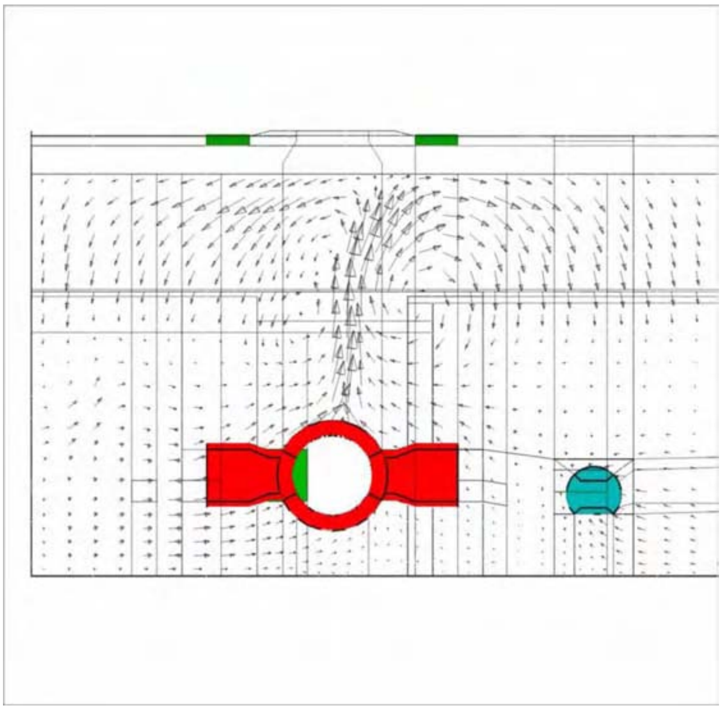

Figure 14: Scenario 1. Velocity vectors at a vertical plane through the axis of the silo combustors under normal operating conditions.

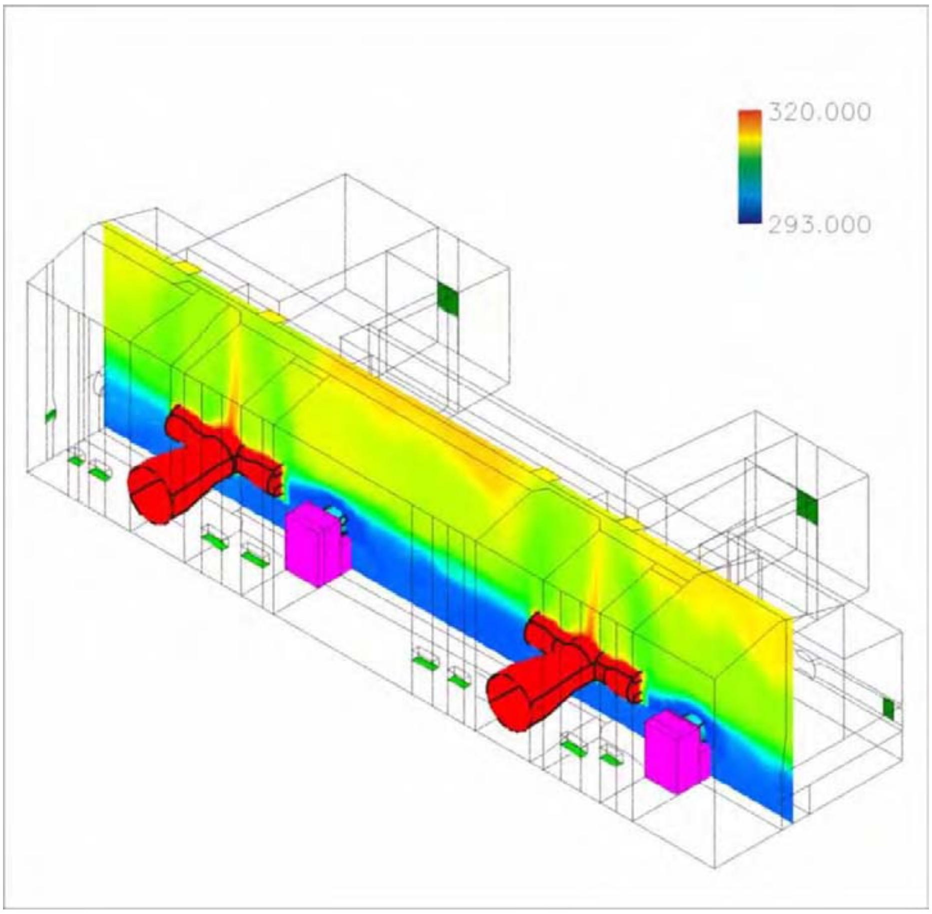

Figure 15: Scenario 1. Temperature field (Kelvin) on a vertical plane through the axis of the silo combustors under normal operating conditions.

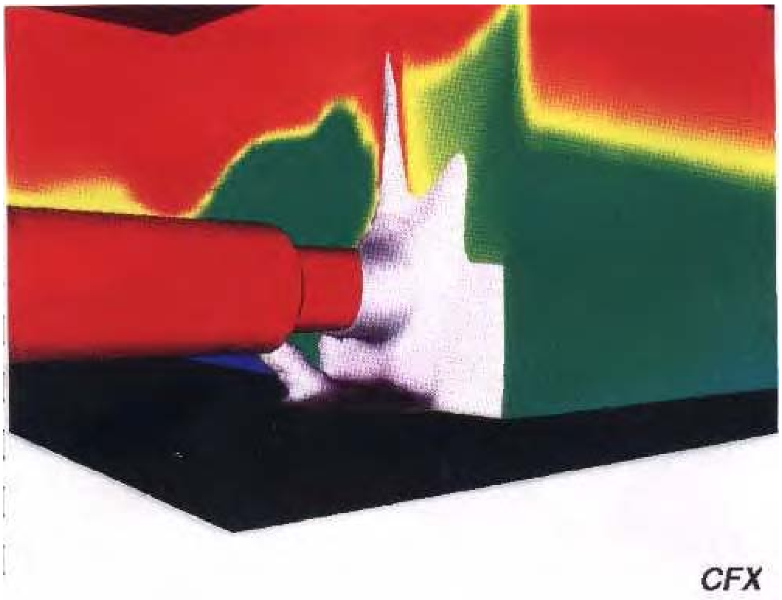

Figure 16: Scenario 2. Gas cloud enclosed by the (grey) 50% LEL iso-surface calculated by AEA Technology (Sinai and Hoyal, 1997).

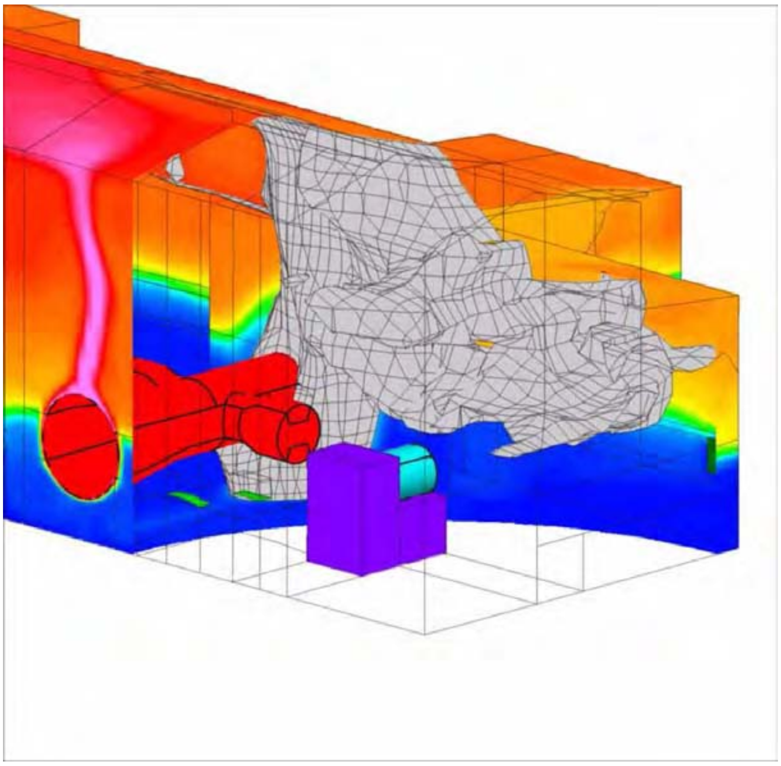

Figure 17: Scenario 2. Gas cloud enclosed by the (grey) 50% LEL iso-surface with the porous region modelled below the gas turbine.

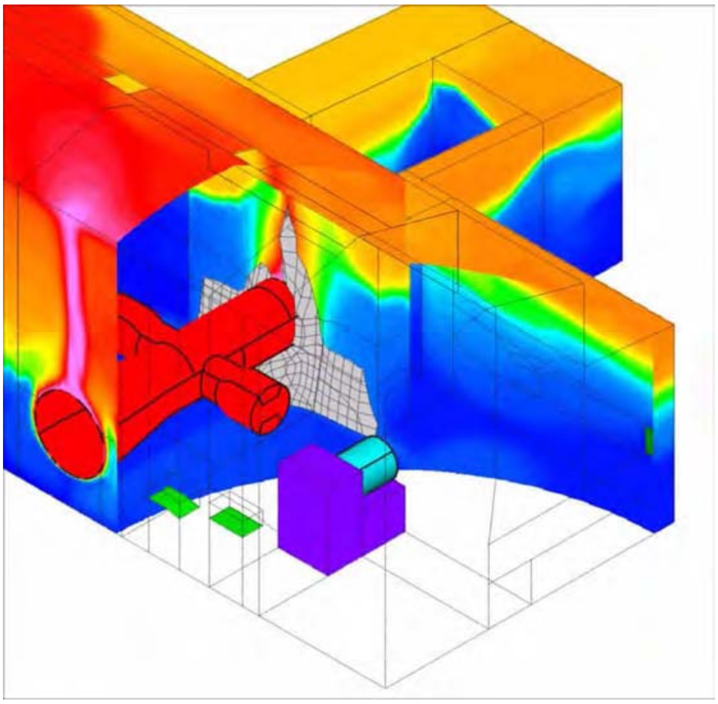

Figure 18: Scenario 2. Gas cloud enclosed by the (grey) 50% LEL iso-surface without the porous region below the gas turbine.

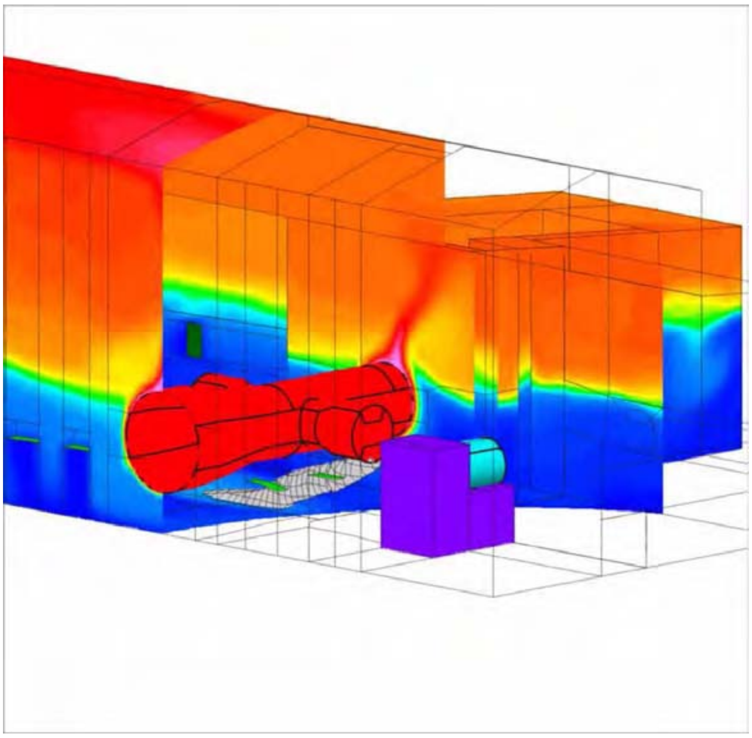

Figure 19: Scenario 3. Gas cloud enclosed by the (grey) 50% LEL iso-surface without the porous region modelled below the gas turbine.

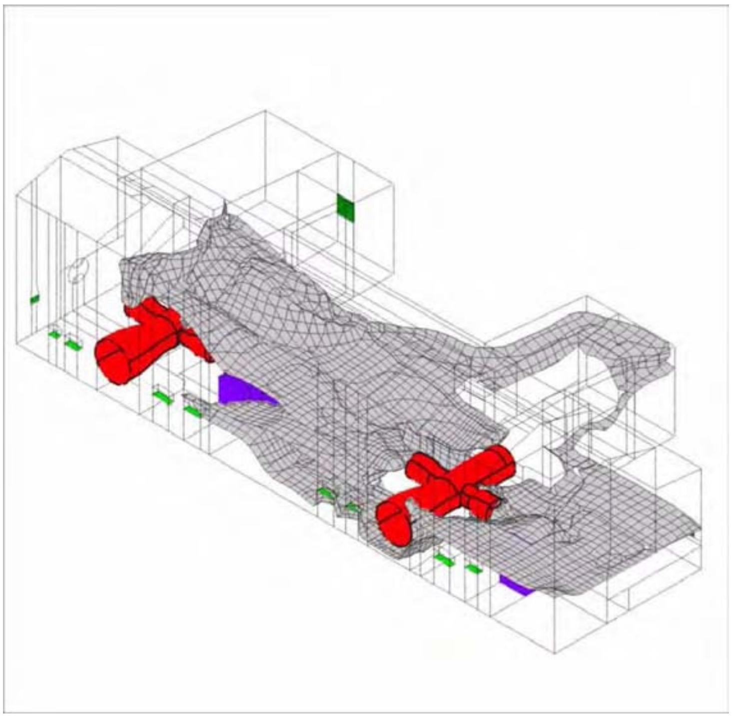

Figure 20: Scenario 3. Gas cloud enclosed by the (grey) 10% LEL iso-surface without the porous region modelled below the gas turbine.

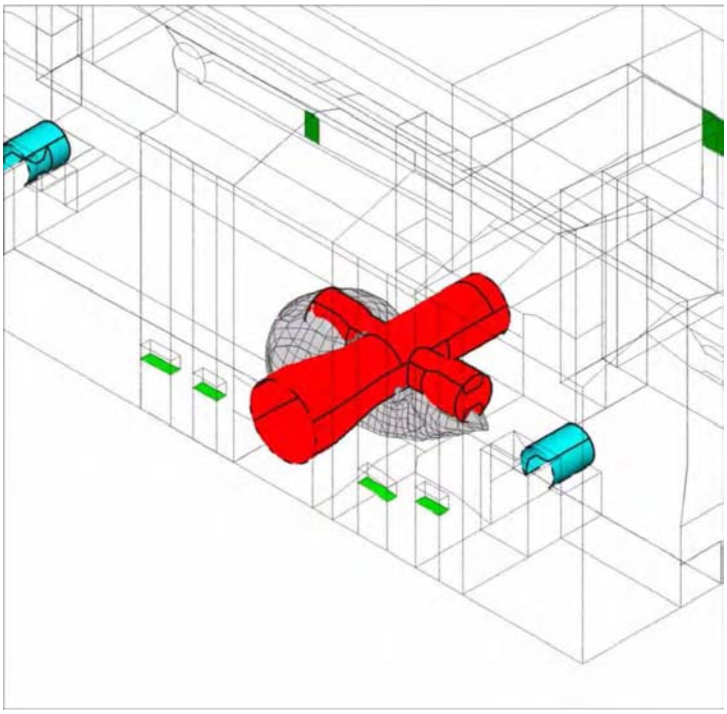

Figure 21: Scenario 4. The transient build-up of the gas cloud at 40s. (The iso-surface is an arbitrary value in the range 10<%LEL<50 for illustrative purposes only).

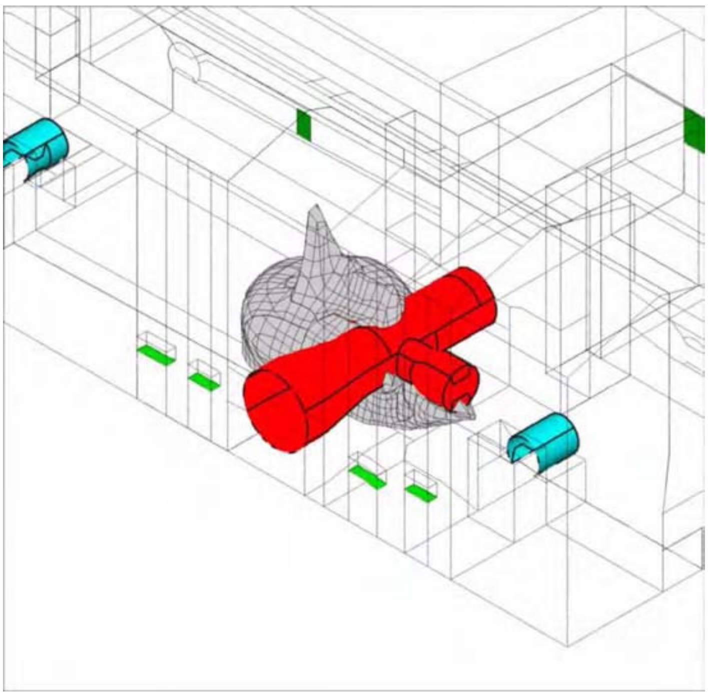

Figure 22: Scenario 4. The transient build-up of the gas cloud at 60s. (The iso-surface is an arbitrary value in the range 10<%LEL<50 for illustrative purposes only).

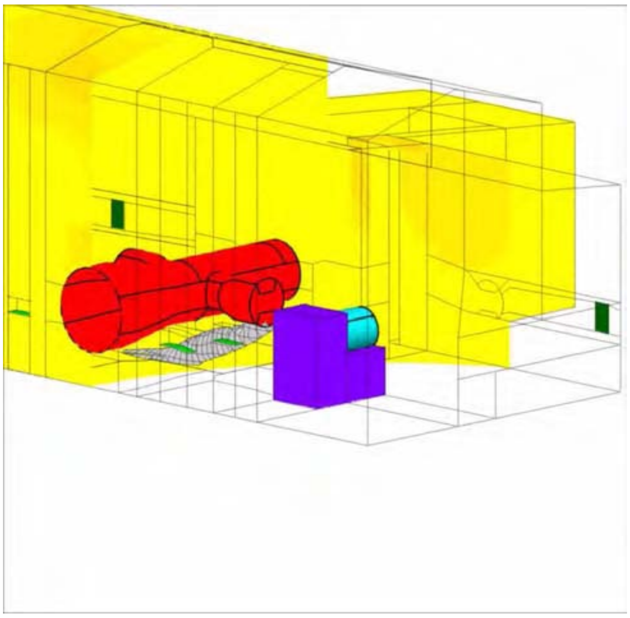

Figure 23: Scenario 5. Gas cloud enclosed by the (grey) 50% LEL iso-surface.

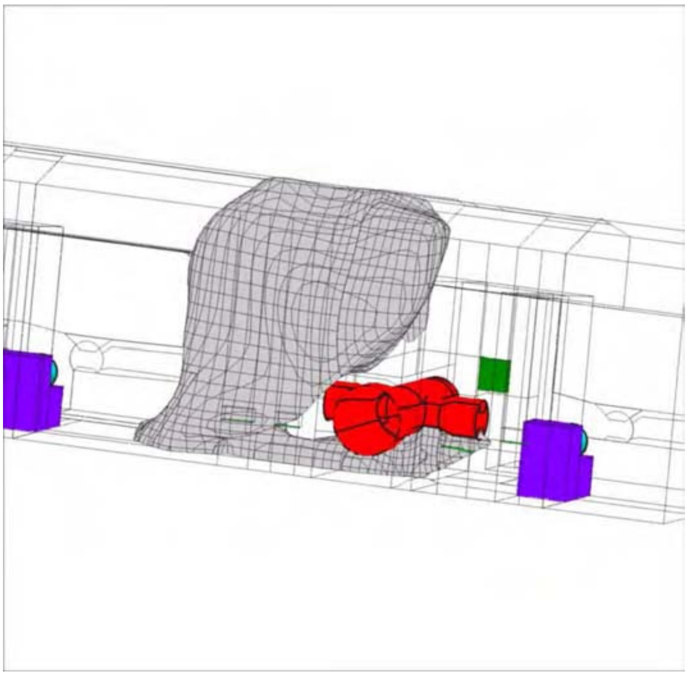

Figure 24: Scenario 5. Gas cloud rising vertically in the centre of the turbine hall. (The iso-surface is an arbitrary value in the range 10<%LEL<50 for illustrative purposes only).

A. Description of measurements taken at Didcot B silo combustor gas turbine hall

Three sets of measurements were taken in the Didcot B silo combustor turbine hall on two separate days. On the first occasion (16 June 1998) a combined hot bulb anemometer and temperature probe was used to take the data shown in Table A1 and Figure A3, at the positions shown in Figures A1 and A2. The hot bulb anemometer provides a measure of the flow speed. Point measurements were taken at a frequency of one a minute over several minutes. The accuracy of the hot bulb anemometer and temperature probe is +/- $0.05ms^{-1}$, +/- $0.1^{o}C$, but this is not maintained at very low velocities of order 0.1m/s.
On the second visit (5 March 1999) both a hot bulb anemometer and an ultrasonic anemometer were used. The latter was employed as it was capable of more accurately resolving very low flow speeds in the region of cm/sec, and additionally it provided a velocity vector by recording the individual flow components. The accuracy of the ultrasonic anemometer is +/-$0.001ms^{-1}$, down to absolute values of this magnitude. Logging rates were typically once every 10 seconds for the hot bulb anemometer, and once a second for the ultrasonic anemometer. In order to obtain a representative indication of fluctations in air flow at the monitoring points the instruments were left recording for periods ranging from 5 minutes to approximately 15 minutes. The sample points and data obtained are given in Tables A2 and A3 and in Figures A4 to A7.
During both visits it was noted that the measurements were strongly influenced by the external environmental conditions. For instance on the first visit, a temperature of approximately 50 ^{o}C was noted on the walkway above the GTs, whereas on the following day - when the measurement survey was undertaken, the temperature had fallen to approximately 40 ^{o}C. Large fluctuations over time were also noted in the flow through the inlets. The type most affected were those consisting of penetrations directly through the wall of the turbine hall (Figure 5). As such, the flow through these inlets varied greatly depending on whether a gust of wind was blowing at the vent at the time. Large variations were also noted over the area of the vent due to the presence of box section baffles in the structure, as well as louvered vents. Additional complications were caused by a number of ill-fitting doors being present in the hall, a number of these were large roller-shutter doors where a gap of up to ~20 mm was seen along a large part of the bottom of the door. In another part of the hall, one door (door A, close to measurement position 1) was often blown open for long periods by a flow of air leaving the hall and passing into an adjacent hall. As a consequence flow in the bulk of the hall was also subject to large fluctuations in both speed and direction.
These difficulties make it hard to draw firm conclusions. Certainly the flow in the hall is strongly influenced by external conditions and is typically of magnitude much less than 1m/s. The day to day difference in the influence of external conditions is evident when comparing flow speed and temperatures in Tables A1 and A2. The large variation in maximum and minimum speed about the mean indicates that flow in the hall is also being perturbed in the short term by the external conditions.
A comparison of measurements made on the same day (5/3/99) with different instruments (Table A2 and A3), reveals that there are significant differences. Flow speeds measured with the ultrasonic anemometer are generally lower than those measured with the hot bulb instrument. In particular values at measuring position 1 differ greatly. However it is noted that door A was largely open for the duration of the hot bulb measurements at this location and could well have been closed for the (later) ultrasonic measurements. The hot bulb measurements at position 1 may thus also be responding to local flows from the turbine hall through door A

into the adjacent hall. Broadly speaking, the degree of correspondence between the ultrasonic and hot bulb flow speeds at the other positions, 3 and 4, is similar.

Overall, it would appear that greater confidence can be placed on flow speeds in the bulk of the hall as measured by the ultrasonic anemometer (Table A3), largely due to its ability to measure down to very low velocities with high accuracy. Unfortunately relatively few measurements were made with this device. Flow speeds measured at the inlet ducts using the hot bulb anemometer can be treated with confidence, since the velocity magnitude is here generally >1m/s, although the above caveats with regard to the influence of external conditions still apply.

Table A1: Temperature and velocity measurements taken on 16/6/98 in module 5, Didcot B power station

Position	Height (m)	Range of flow speed (m/s)	Temperature (^{0}C)
1	5	0.18 - 0.66	35.5
	10	0.14 - 0.74	41.4
	15.2	0.16 - 0.23	44.4
2	5	0.29 - 0.49	33.6
	10	0.28 - 0.33	42.1
	15.2	0.09 - 0.15	44.4
2A	5	0.25 - 0.62	33.8
	10	0.20 - 0.43	43
	15.2	0.14 - 0.30	44.9
2C	5	0.20 - 0.65	34.8
	10	0.03 - 0.14	42.2
3	5	0.22 - 0.64	33.5
	10	0.03 - 0.33	41.9
	15.2	0.28 - 0.35	45.6
3A	5	0.02 - 0.07	33
	10	0.17 - 0.37	41.1
4	5	0.35 - 0.70	34.5
	10	0.09 - 0.25	42.5
5	5	0.25 - 0.59	35.3
	10	0.15 - 0.65	42.0
	15.2	0.15 - 0.29	45.1
GT 1	10.5	0.75 - 1.25	46.6
GT 2	10.5	0.9 - 1.4	46.4
A	5	0.12 - 0.20	35.8
B	5	0.03 - 0.06	33.9
C	5	0.07 - 0.15	36.1
D	5	0.02 - 0.10	35

Table A2: Hot bulb temperature and velocity measurements in module 5, Didcot B power station, taken on 5/3/99.

Position	Height (m)	Mean flow speed and standard deviation (m/s)	Min. flow speed (m/s)	Max. flow speed (m/s)	Temperature (^{0}C)	Direction of flow where evident
1	5.8	0.97 ± 0.21	0.38	1.22	26.9	Towards Door A
	9.8	0.79 ± 0.17	0.25	1.2	31.5	Towards Door A
	16	0.18 ± 0.08	0.04	0.34	35.4	-
3	5.8	0.50 ± 0.05	0.41	0.64	25.7	-
	9.8	0.17 ± 0.07	0.08	0.31	33.7	-
	16	0.19 ± 0.07	0.07	0.41	36.1	-
4	5.8	0.47 ± 0.09	0.35	0.56	27.6	-
	9.8	0.36 ± 0.10	0.20	0.64	34.9	-
	16	0.33 ± 0.15	0.09	0.81	36.2	-
GT 1	10.5	1.19 ± 0.14	1.01	1.36	37.3	Upwards
GT2	10.5	1.61 ± 0.20	1.14	1.88	40.2	Upwards
Door A (open by 20 cm)	1.3-1.5	0.53 ± 0.32	0.40	1.25	22.5 - 21	Into next module (heat recovery steam generator building)
Door A (shut)	1.3-1.5	0.31 ± 0.32	0.12	0.56	17 - 18	"
Door B (improperly shut door in rollershutter door)	1.3-1.5	0.31 ± 0.05	0.26	0.40	16 - 18	Into turbine hall
Door C (approx 2 cm gap under roller-shutter door)	0	0.74 ± 0.25	0.36	1.18	14	Into turbine hall
Door D	1.3-1.5	0.11 ± 0.06	0.06	0.28	18	Into turbine hall

Table A3:Ultrasonic anemometer speed and velocity measurements at Didcot B power station, data of 5/3/99.

Position	Height(m)	Mean flow speed (m/s)	Standard deviation	Maximum flow speed (m/s)	Minimum flow speed (m/s)	U* (m/s)	V* (m/s)	W* (m/s)
1	5.8	0.15	0.07	0.41	0.02	0.07	-0.02	-0.05
	9.8	0.17	0.11	0.68	0	0.02	-0.06	-0.03
3	5.8	0.23	0.05	0.39	0.12	0.16	-0.14	0
	9.8	0.19	0.06	0.45	0.05	0.02	-0.17	0.03
4	5.8	0.36	0.07	0.69	0.11	0.21	-0.27	0
	9.8	0.23	0.07	0.44	0	0.14	-0.14	0.04

* See Figure A4 for orientation

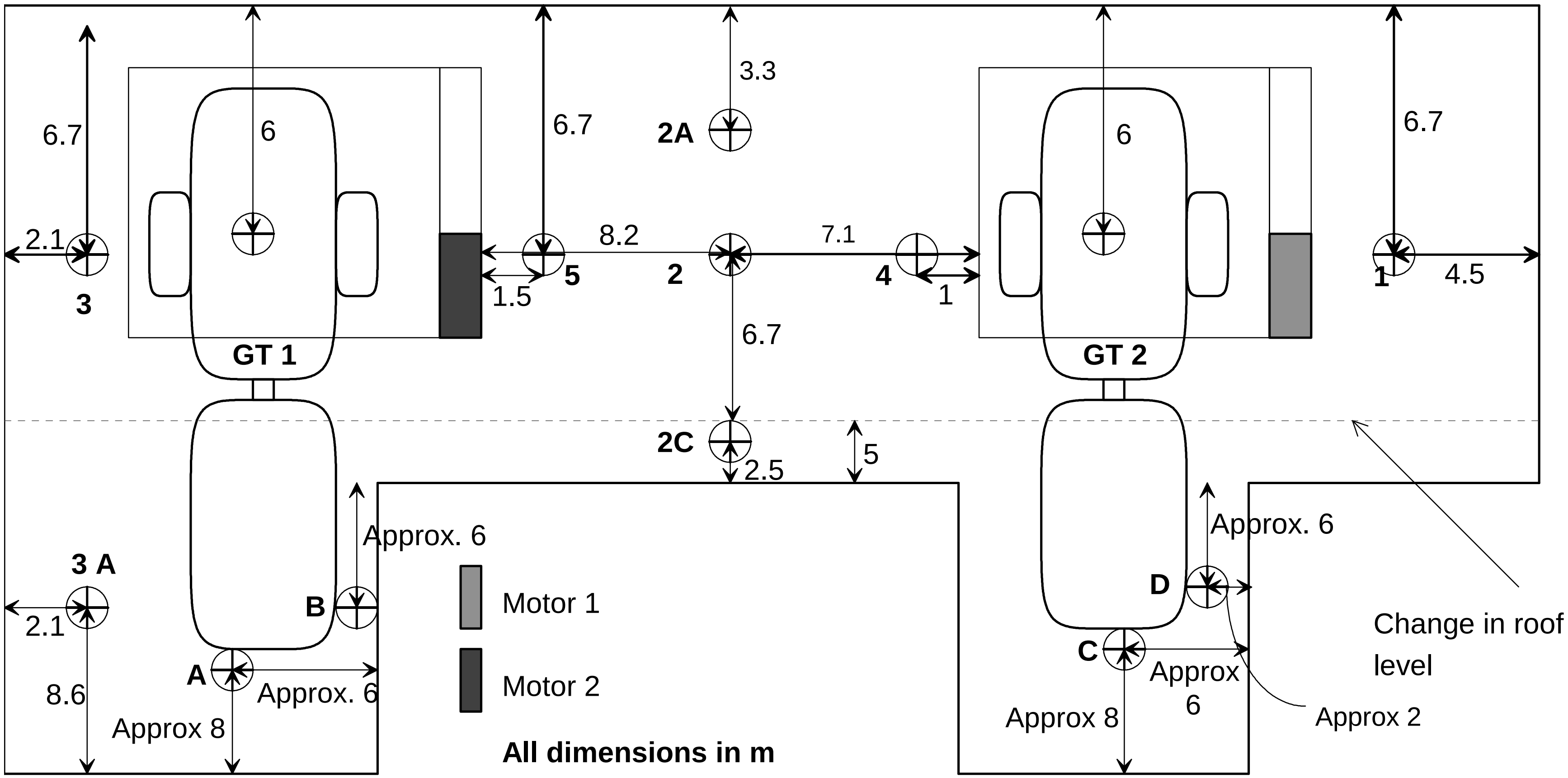

Figure A1: Measurement Positions for data taken on 16/6/98.

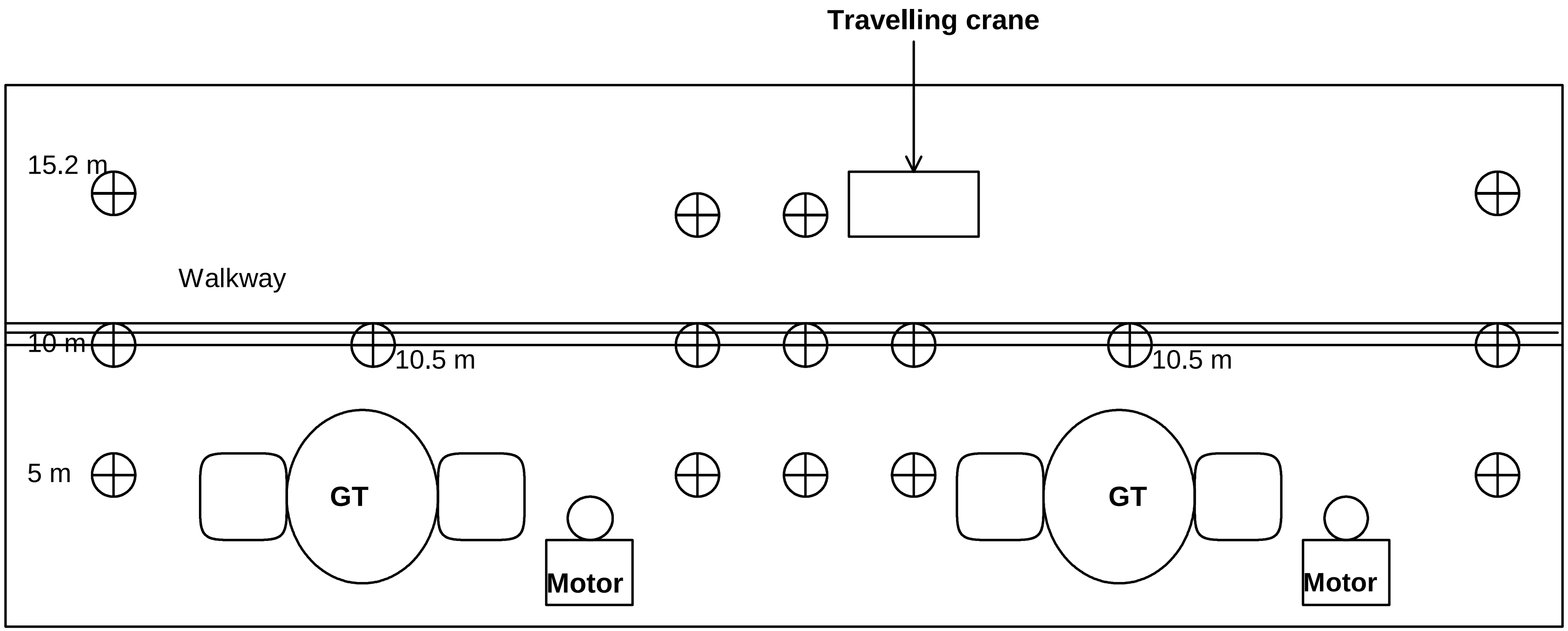

Figure A2: Side view of turbine hall showing measurement positions for velocities and temperature, 16/6/98.

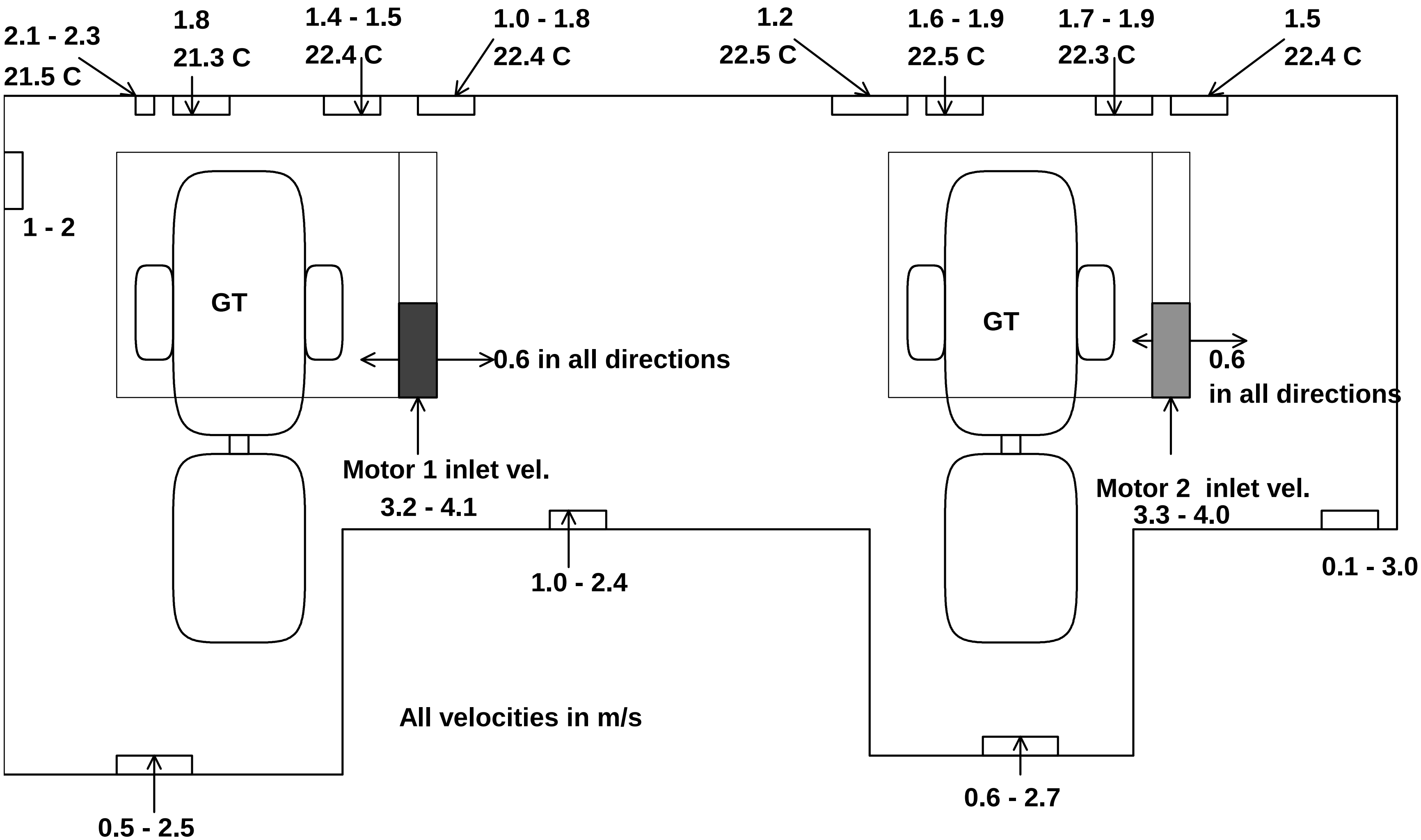

Figure A3: Measured inlet velocities and temperatures, and velocities near motors, taken on 16/6/98.
(Velocity values indicated are minima & maxima)

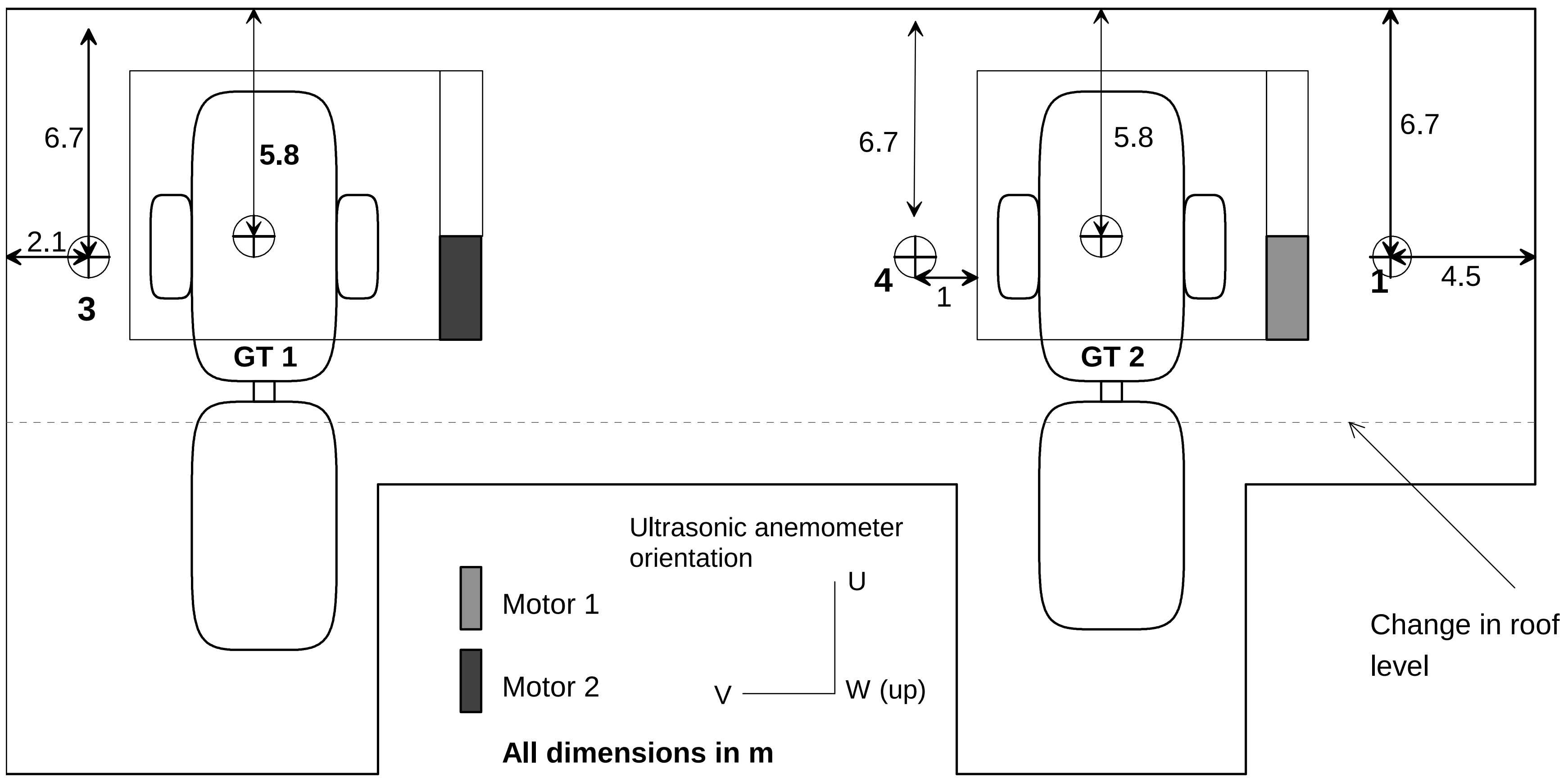

Figure A4: Measurement positions for data taken on 5/3/99.

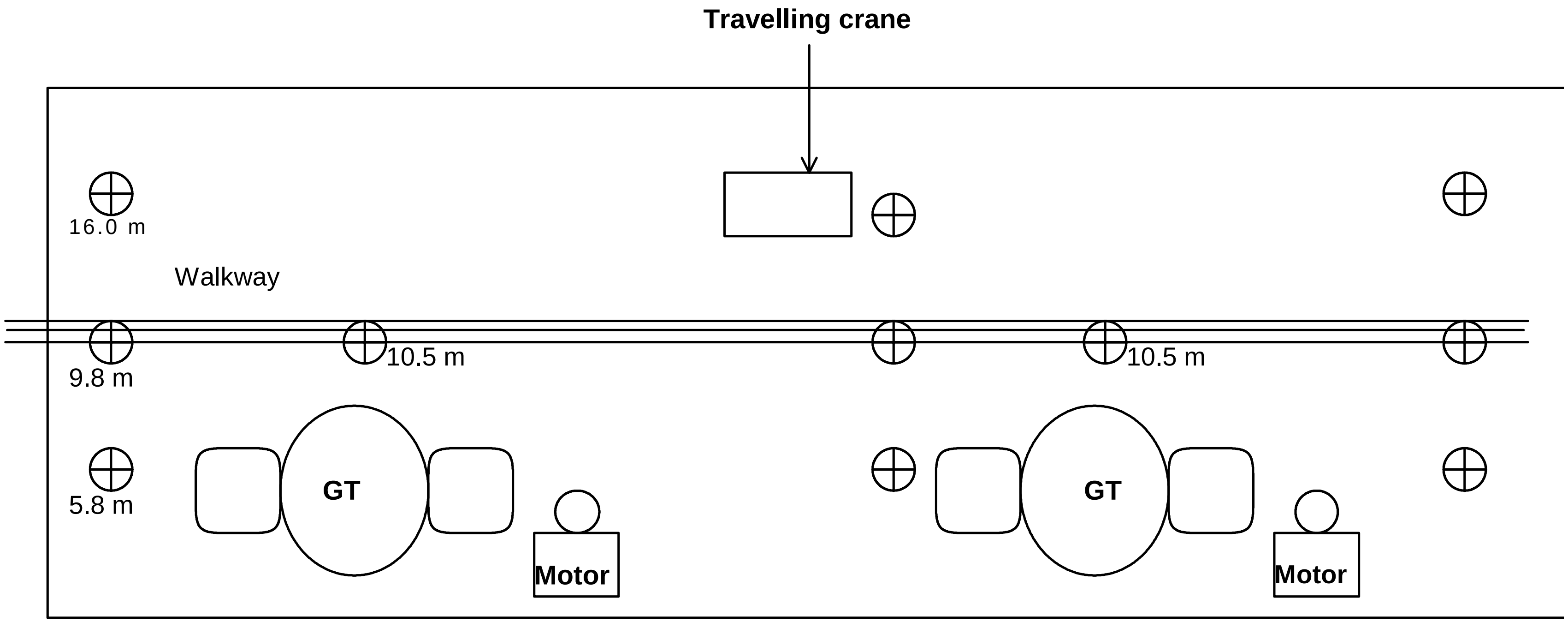

Figure A5: Side view of turbine hall showing measurement positions for velocity & temperature data taken on 5/3/99

Figure A6: Inlets and doorways into turbine hall, hot bulb flow measurements taken on 5/3/99.

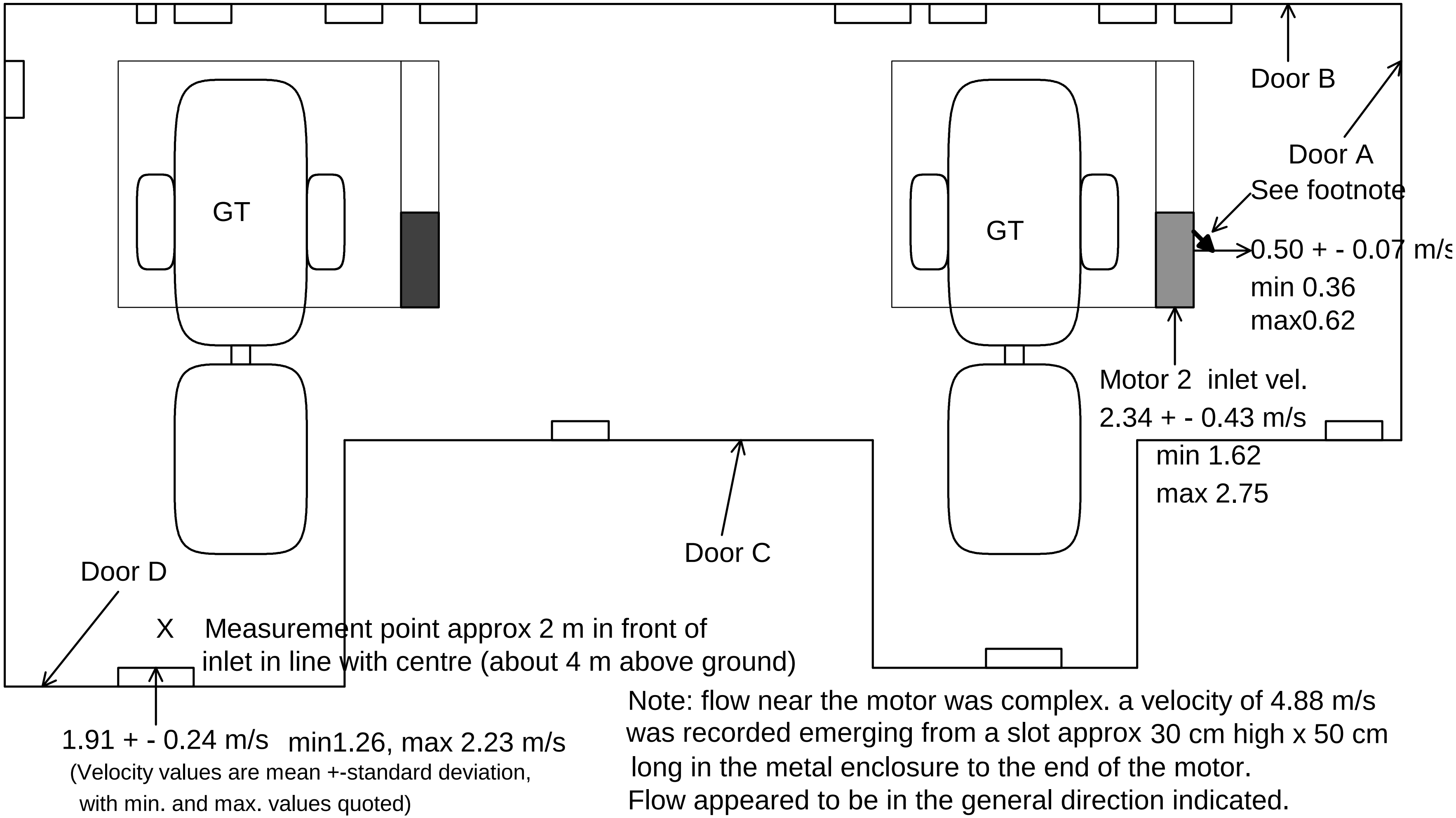

Figure A7: Surface temperature measurements taken on 5/3/99